Defect and Diffusion Forum
ISSN: 1662-9507, Vol. 374, pp 29-46
doi:10.4028/www.scientific.net/DDF.374.29
© 2017 Trans Tech Publications, Switzerland
Submitted: 2017-01-18
Revised: 2017-02-10
Accepted: 2017-02-10
Online: 2017-04-21

Thermodynamics Analysis of Unsteady MHD Mixed Convection with Slip and Thermal Radiation over a Permeable Surface

A. Muhammad[1,a], O. D. Makinde[2,b*],

[1]Department of Applied and Theoretical Physics, African University of Science and Technology, Abuja, Nigeria

[2]Faculty of Military Science, Stellenbosch University, Private Bag X2, Saldanha 7395, South Africa

[a]ahmadmuhammad325@gmail.com, [b]makinded@gmail.com

Keywords: Permeable surface, hydromagnetic flow, suction/injection, buoyancy force, thermal radiation, entropy generation

Abstract. This paper discusses the thermodynamics irreversibility in an unsteady hydromagnetic mixed convective flow of an electrically conducting optically dense fluid over a permeable vertical surface under the combined influence of thermal radiation, velocity slip, temperature jump, buoyancy force, viscous dissipation, Joule heating and magnetic field. The governing partial differential equations are reduced to ordinary differential equations by using similarity variable. A local similarity solution is obtained numerically using shooting technique coupled with Runge-Kutta Fehlberg integration method. The influence of various thermophysical parameters on velocity and temperature profiles, skin friction, Nusselt number, entropy generation rate and Bejan number are presented graphically and discussed quantitatively. It is found that velocity slip, surface injection and temperature jump can successfully reduce entropy generation rate in the presence of an applied magnetic field. A comparison of numerical solution is made with the exact solution under a special case scenario and excellent agreement is found.

Introduction

Theoretical study of magnetohydromagnetic (MHD) mixed convective flow and heat transfer over a permeable surface in the presence of slip and radiative heat absorption appears to be increasingly important due to its various applications in engineering and industries processes, especially in field of micro-electro-mechanical-systems (MEMS), such as micro MHD pumps, micro-electronic devices, rapid mixing of fluids in biological processes, biological transportation, and drug delivery [1-3]. MHD occurs due to mutual interaction between magnetic field and electrically conducting fluid flowing across it. The applied magnetic field generates Lorenz force that controls the electrically conducting fluid flow in a mixing process. Most of the applications of magnetic field in the biological transportation are in the micro/nano systems. Therefore, it is necessary to consider the influence of the velocity slip at the boundaries [4]. Surface permeability is another important aspect in micro-mixing of biological fluid. This enables transpiration process to take place at the boundaries in a micro system. In this process, suction is exerted in order to remove reactants, whereas injection is applied to add reactants in the process [5]. Hydromagnetic flow with heat transfer also play a very vital role in the design of cooling systems for electronic devices, MHD generators, plasma studies, nuclear reactors cooling, geothermal energy extraction, solar energy collection, MHD marine propulsion, electronic packages, gas turbines, exchangers placed in a low-velocity environment, various propulsion devices for aircraft, missiles, satellites and space vehicles, thermal insulation, and petroleum reservoirs. Moreover, many processes in engineering do occur at high temperatures and the knowledge of radiative heat transfer becomes very important, particularly in designing pertinent equipment [6-8]. Thermal radiation is the emission of electromagnetic waves from all matter that has a temperature greater than absolute zero. The effects of radiation also become more important when the difference between the surface and the ambient temperature is large. Several excellent studies on hydromagnetic boundary layer flows with heat transfer have been communicated by many authors [9-12]. Mukhopadhyay [13] investigated the slip effects on MHD

All rights reserved. No part of contents of this paper may be reproduced or transmitted in any form or by any means without the written permission of Trans Tech Publications, www.ttp.net. (#87860788-22/04/17,13:12:22)

boundary layer flow by an exponentially stretching sheet with suction/blowing and thermal radiation. The combined effects of variable thermal conductivity, viscous dissipation and Ohmic heating on MHD natural convection flow of low Prandtl fluid over an inclined porous plate was studied by Sharma and Singh [14]. Kim [15] reported a numerical solution for the unsteady MHD convective heat transfer past a semi-infinite vertical porous moving plate with variable suction. Bhattacharyya and Layek [16] discussed the problem of chemically reactive solute distribution in hydromagnetic boundary layer flow over a permeable stretching sheet with suction or blowing. The combined effects of velocity slip and temperature jump on hydromagnetic boundary layer flow of an electrically conducting fluid over a porous shrinking surface was numerically investigated by Zheng *et al.* [17]. The mixed convection of a conducting fluid with thermal radiation and thermophoresis effects on a vertical flat plate embedded in a porous medium has been studied by Kishan and Jagadha [18]. Other relevant studies existing in the literature with respect to hydromagnetic effects on boundary layer flows of a conducting fluid with or without porous medium can found in [19-21].

Meanwhile, the recent trend in the study of fluid flow with heat transfer characteristics is related to the concept of entropy generation minimization. The foundation of knowledge of entropy production goes back to Clausius and Kelvin's studies on the irreversible aspects of the second law of thermodynamics [22]. Entropy generation is associated with thermodynamic irreversibility, and is common to all types of fluid flow with heat transfer processes. Efficient utilization of energy is the primary objective in the design of any thermodynamic system. This can be achieved by minimizing entropy generation in the system, since entropy production destroys the available energy. The core interest in thermodynamic irreversibility analysis is to determine the factors responsible for the entropy generation and minimise their effects in order to avoid the energy losses and fully utilize the available energy resources. Such information can also be employed to improve the design of flow and thermal systems for efficient operation. Bejan [23, 24] introduced the theoretical concept of entropy generation minimization with respect to fluid flow with heat transfer characteristics. Thereafter, several researchers [25-28] have investigated the problem under various physical situations. They showed that the pertinent flow parameters might be chosen in order to minimize entropy generation inside the system. Chinyoka and Makinde [29] numerically studied the entropy generation rate in an unsteady porous channel flow with Navier slip and convective cooling. Mahmud and Frazer [30] studied the effect of viscous dissipation on entropy generation characteristic inside a porous channel. Makinde and Beg [31] applied the second law analysis to the problem of inherent irreversibility in a reactive hydromagnetic channel flow. The entropy generation rate in hydromagnetic boundary layer flow over a convectively heated flat surface was analysed by Makinde [32]. Yazdi *et al.* [33] numerically investigated the problem of entropy production in an electrically conducting fluid flowing over open parallel microchannels embedded in a micro-patterned permeable surface in the presence of an externally imposed magnetic field. They reported that microchannels embedded in a micro-patterned permeable surface can successfully reduce entropy generation in the presence of an applied magnetic field.

There have been numerous analytical or numerical solutions in the literature developed particularly for entropy generation analysis of boundary layer flow. However, to the best of our knowledge, no research has have been done yet to analyze the combined effects of velocity slip, buoyancy force, temperature jump, thermal radiation absorption, viscous and Joule heating on local entropy production in unsteady MHD fluid flow with heat transfer over a permeable surface. Therefore, our objective is to tackle this problem numerically using shooting technique coupled with Runge-Kutta Fehlberg integration method. This study essentially extends the earlier work of Makinde [25] and Yazdi *et al.* [33] to unsteady MHD boundary layer flow with inclusion of thermal radiation, suction/injection, temperature jump, buoyancy force and Joule heating. The influence of various thermophysical parameters on the flow velocity, temperature profiles, friction factor and local Nusselt number along with the entropy generation rate and Bejan number are discussed with the help of graphs and tables. The presented study may be applied to a variety of flow and thermal systems including micro scale systems such as micro-mixing technologies.

Model Formulation

We consider an unsteady mixed convective flow of an incompressible, electrically conducting and optically dense fluid over a vertical surface. It is assumed that the plate surface is permeable, fixed, slippery and may be subjected to fluid suction or injection. The *x*-axis is along the plate surface and *y*-axis is orthogonal to it. A magnetic field of strength H_0 is applied normal to the plate surface and the magnetic Reynolds number is assumed to be small so that the induced magnetic field can be neglected in comparison with the applied magnetic field. The physical flow model and coordinate system is shown in figure 1 below,

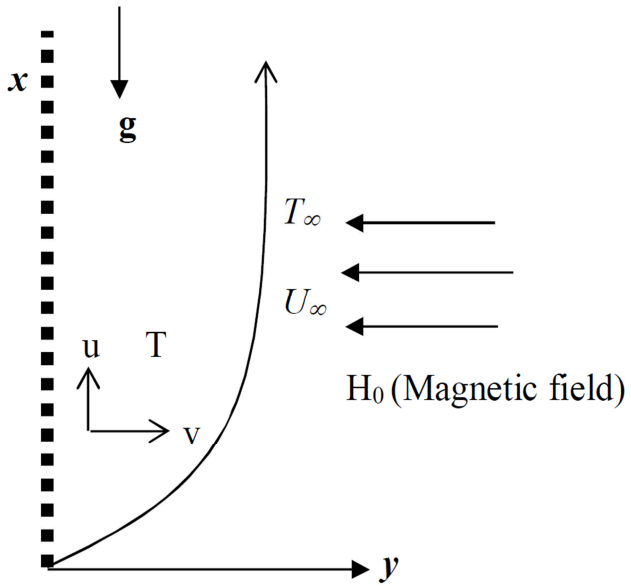


Fig. 1: Problem geometry.

The heat transfer analysis is carried out in the presence of thermal radiation absorption, Joule and viscous heating. Under the usual boundary layer approximations, the governing equations of continuity, momentum with Oberbeck-Boussinesq approximations for the buoyancy forces, and thermal energy can be expressed as [7-9, 13-17]:

$$\frac{\partial v}{\partial y} = 0, \tag{1}$$

$$\frac{\partial u}{\partial t} + v\frac{\partial u}{\partial y} = \upsilon\frac{\partial^2 u}{\partial y^2} - \frac{\sigma {H_0}^2}{\rho}(u-U) + g\beta(T-T_\infty), \tag{2}$$

$$\frac{\partial T}{\partial t} + v\frac{\partial T}{\partial y} = \alpha\frac{\partial^2 T}{\partial y^2} + \frac{\upsilon}{c_p}(\frac{\partial u}{\partial y})^2 + \frac{\sigma {H_0}^2}{\rho c_p}(u-U)^2 - \frac{1}{\rho c_p}\frac{\partial q_r}{\partial y}, \tag{3}$$

with the boundary conditions for time $t > 0$ given as,

$$u = L\frac{\partial u}{\partial y},\ T = T_w + m\frac{\partial T}{\partial y},\ \text{at}\quad y = 0, \tag{4}$$

$$u \to U,\ T \to T_\infty,\quad \text{as } y \to \infty \tag{5}$$

where (*u, v*) are the velocity components in the *x* and *y* directions respectively, *m* is the temperature jump, *L* denotes the velocity slip length, *k* is the fluid thermal conductivity coefficient, υ is the kinematic viscosity, ρ is the density, *U* is the free stream velocity, β is volumetric thermal expansion coefficient, *g* is the acceleration due to gravity, *T* is the temperature, T_w is the plate surface temperature, T_∞ is the free stream temperature, α is the thermal diffusivity and c_p is the specific heat at constant pressure. By using the Rosseland approximation ([6-8, 18, 21]) for thermal radiation in an optically thick layer, the radiative heat flux q_r is given as

$$q_r = -\frac{4\sigma^*}{3k^*}\frac{\partial T^4}{\partial y} \approx -\frac{16\sigma^* T_\infty^3}{3k^*}\frac{\partial T}{\partial y}, \tag{6}$$

where $T^4 \cong 4T_\infty^3 T - 3T_\infty^4$ by Taylor series approximation, σ^* is the Stefan–Boltzmann constant, k^* is the mean absorption coefficient. The continuity equation (1) shows that the normal velocity v is either constant or a function of time. We therefore choose the time dependent normal velocity as

$$v = -b\left(\frac{\upsilon}{t}\right)^{\frac{1}{2}}, \tag{7}$$

where $b > 0$ is the suction parameter. We introduce the following similarity variables and dimensionless quantities, i.e.

$$\eta = \frac{y}{2\sqrt{\upsilon t}}, u = Uf(\eta),\ \theta = \frac{T - T_\infty}{T_w - T_\infty},\ \Pr = \frac{\upsilon}{\alpha},$$
$$M = \frac{4t\sigma H_0^2}{\rho}, Ec = \frac{U^2}{c_p(T_w - T_\infty)}, \delta = \frac{m}{2\sqrt{\upsilon t}}, \tag{8}$$
$$\lambda = \frac{L}{2\sqrt{\upsilon t}}, Nr = \frac{16\sigma^* T_\infty^3}{3kk^*}, Gr = \frac{4tg\beta(T_w - T_\infty)}{U}.$$

Substituting equations (6)-(8) into equations (2)-(5), we obtain

$$f'' + 2(\eta + b)f' - M(f - 1) + Gr\,\theta = 0, \tag{9}$$
$$(1 + Nr)\theta'' + 2\Pr(\eta + b)\theta' + \Pr\, Ec\left[(f')^2 + M(f - 1)^2\right] = 0, \tag{10}$$

subject to the boundary conditions;

$$f(0) = \lambda f'(0),\quad \theta(0) = 1 + \delta\theta'(0), \tag{11}$$
$$f(\infty) = 1,\quad \theta(\infty) = 0, \tag{12}$$

where prime symbol indicates derivative with respect to η, Pr is the Prandtl number, δ is the temperature jump parameter, M is the magnetic field parameter, Ec is the Eckert number, Gr is the local Grashof number, Nr is the thermal radiation parameter and λ is the velocity slip parameter. Moreover, the exact solution for the equation (9) to (12) exist for the special flow and heat transfer case when M=Gr=Ec=0, and we obtain,

$$f(\eta) = \frac{2\lambda e^{-b^2} + \sqrt{\pi}\left[erf(\eta + b) - erf(b)\right]}{2\lambda e^{-b^2} + \sqrt{\pi}\left[1 - erf(b)\right]}, \tag{13}$$

$$\theta(\eta) = \frac{\sqrt{\pi\Pr(1 + Nr)}\left[erf\left(\frac{\Pr(\eta + b)}{\sqrt{\Pr(1 + Nr)}}\right) - 1\right]}{\sqrt{\pi\Pr(1 + Nr)}\left[erf\left(\frac{\Pr b}{\sqrt{\Pr(1 + Nr)}}\right) - 1\right] - 2\Pr\delta e^{-\frac{\Pr b^2}{1 + Nr}}}. \tag{14}$$

Other physical quantities of engineering and industrial interest in this study are the skin friction coefficient C_f and the local Nusselt number Nu defined respectively as,

$$C_f = \frac{2t\tau_w}{\rho U\sqrt{\upsilon t}} = f'(0), \tag{15}$$
$$Nu = \frac{2q_w\sqrt{\upsilon t}}{k(T_w - T_\infty)} = -(1 + Nr)\theta'(0), \tag{16}$$

where the τ_w and q_w are the local shear stress and the local heat transfer rate at the permeable surface respectively. They are given as

$$\tau_w = \rho\upsilon\left.\frac{\partial u}{\partial y}\right|_{y=0},\ q_w = -k\left(1 + \frac{16\sigma^* T_\infty^3}{3kk^*}\right)\left.\frac{\partial T}{\partial y}\right|_{y=0}. \tag{17}$$

Entropy Analysis

The inherent irreversibility in a hydromagnetic flow of a conducting fluid over a permeable surface may arise due to the exchange of energy and momentum within the fluid and the solid boundaries. Consequently, entropy production may occur as a result of fluid friction, magnetic field and heat transfer in the direction of finite temperature gradients. According to Wood [28], the expression for the volumetric entropy generation rate is given as

$$E_G = \underbrace{\frac{k}{T_\infty^2}\left(1+\frac{16\sigma^* T_\infty^3}{3k^* k}\right)\left(\frac{dT}{dy}\right)^2}_{\substack{\text{entropy effects due to heat}\\ \text{transfer and thermal}\\ \text{radiation absorption}}} + \underbrace{\frac{\rho\upsilon}{T_\infty}\left(\frac{du}{dy}\right)^2}_{\substack{\text{entropy effects}\\ \text{due to fluid}\\ \text{friction}}} + \underbrace{\frac{\sigma B_0^2 (u-U)^2}{T_\infty}}_{\substack{\text{entropy effects}\\ \text{due to magnetic}\\ \text{field}}} \tag{18}$$

and in dimensionless form, we have

$$Ns = \frac{4T_\infty^2 t\upsilon E_G}{k(T_w - T_\infty)} = (1+Nr)(\theta')^2 + \frac{Br}{\Omega}\left[(f')^2 + M(f-1)^2\right] \tag{19}$$

where Br (=$PrEc$) is the Brinkmann number and Ω = (T_w-T_∞) /T_∞ is the temperature difference parameter and $Br\Omega^{-1}$ is referred to as the dimensionless group parameter. $Br\Omega^{-1}$ represents the effect of viscous and Joule heating due to the combined action of fluid friction and magnetic field on the entropy generation rate. The Bejan number is defined as the ratio of heat transfer irreversibility to total irreversibility due to heat transfer, fluid friction and magnetic field for the laminar MHD boundary layer flow. The Bejan number Be is given by [22-28]:

$$Be = \frac{N_1}{Ns} = \frac{1}{1+\Phi} \quad , \tag{20}$$

where

$N_1 = (1+Nr)(\theta')^2$, (is the thermal radiation and heat transfer irreversibility),

$N_2 = \frac{Br}{\Omega}\left[(f')^2 + M(f-1)^2\right]$ (is the fluid friction and magnetic field irreversibility),

$\Phi = \frac{N_2}{N_1}$, (is the irreversibility ratio).

The Bejan number ranges from 0 to 1, it approaches zero when the entropy generation due to the combined effects of fluid friction and magnetic field is dominant. When Be =0.5 both N_1 and N_2 contribute equally to the entropy generation in the flow process. As Be > 0.5, the irreversibility due to thermal radiation absorption and heat transfer dominate and Be = 1 is the limit at which the irreversibility is solely due to thermal radiation and heat transfer. Consequently, $0 \le \Phi \le 1$ indicates that the irreversibility is primarily due to the thermal radiation and heat transfer irreversibility, whereas for $\Phi > 1$ it is due to the sum of the fluid friction and magnetic field irreversibility. The entropy generation rate, Ns in equation (19) together with Bejan number in equation (20) will be used for the evaluation of the present study.

Numerical Procedure

The dimensionless model equations (9)-(10) together with the boundary conditions (11)-(12) represent a boundary value problem (BVP) and are transformed into a set of nonlinear first order ordinary differential equations with some unknown initial conditions to be determined by shooting technique. Let,

$$f = y_1\ , f' = y_2, \theta = y_3\ , \theta' = y_4. \tag{21}$$

The governing equations then become

$$\left.\begin{aligned} y_1' = y_2,\ \ y_2' = -2(\eta + b)y_2 + M(y_1 - 1) - Gry_3, \\ y_3' = y_4,\ y_4' = -\frac{1}{(1+Nr)}\left[2\,\mathrm{Pr}(\eta + b)y_4 + \mathrm{Pr}\,Ec\left(y_2^2 + M(y_1 - 1)^2\right)\right], \end{aligned}\right\} \tag{22}$$

with the corresponding initial conditions as

$$y_1(0) = -\lambda y_2(0),\ \ y_2(0) = a_1,\ \ y_3(0) = 1 + \delta y_4(0),\ \ y_4(0) = a_2. \tag{23}$$

The unknown initial conditions a_1, a_2 are first guessed and subsequently determined using Newton-Raphson's method for each set of parameter values with respect to the prescribed boundary conditions. The resulting initial value problem is numerically solved using a fourth order Runge-Kutta-Fehlberg integration scheme [34]. The step size is taken as $\Delta\eta = 0.001$ and the convergence criterion was set to 10^{-6}. In practice, $\eta = \infty$ must be replaced by an approximation $\eta = \eta_{max}$, where η is arbitrary as long as it is chosen large enough so that the prescribed free stream conditions are smoothly satisfied. From the process of numerical computation, we obtain the local skin friction (C_f), the local Nusselt number (Nu), the entropy generation rate and the Bejan number as given by equations (15) –(16) and (19)-(20).

Results and Discussions

Here, we discuss the influence of various thermophysical parameters involved in the present problem on the flow and thermal field along with entropy generation characteristics. For most of the computational results (except where stated), the value of the Prandtl number is chosen to be Pr = 0.72, which represents air at 25^0C and one atmospheric pressure. Attention is focused on positive values of the buoyancy parameter (i.e., local thermal Grashof number $Gr > 0$) which corresponds to the cooling problem). The cooling problem is often encountered in engineering applications, for example, in the cooling of electronic components and nuclear reactors. The values of other parameters are fixed arbitrarily for computational purpose. Table 1 shows a comparison between the results obtained from the exact solution of a special flow and heat transfer case when $M = Gr = Ec = 0$ and that of pure numerical approach based on shooting technique coupled with Runge-Kutta-Fehlberg integration scheme. It is noteworthy that the results obtained for shows excellent agreement and this serves as a benchmark for the accuracy of our numerical procedure.

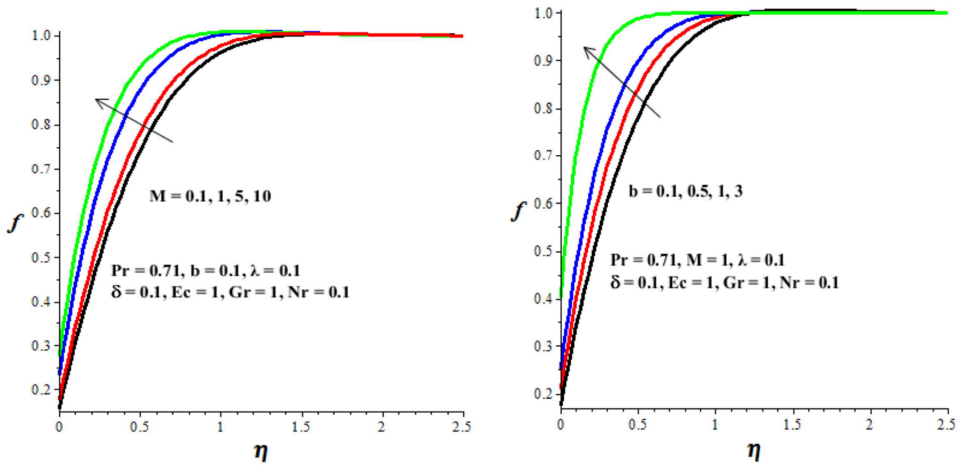
Table 1: Comparison between the exact and numerical solutions for Gr = M = Ec= 0, Pr=0.72, Nr=0.1, b=0.1.

λ	δ	$f'(0)$ Exact Solution	$-\theta'(0)$ Exact Solution	$f'(0)$ Numerical Solution	$-\theta'(0)$ Numerical Solution
0.1	0.1	1.1179876	0.90730785	1.11798758	0.907307855
0.2	0.2	1.0055665	0.83183482	1.00556650	0.831834828
0.3	0.3	0.9136889	0.76795375	0.91368899	0.767953759
0.4	0.4	0.8371954	0.71318448	0.83719537	0.713184488
0.5	0.5	0.7725203	0.66570727	0.77252033	0.665707278
0.7	0.7	0.6691361	0.58748823	0.66913608	0.587488239

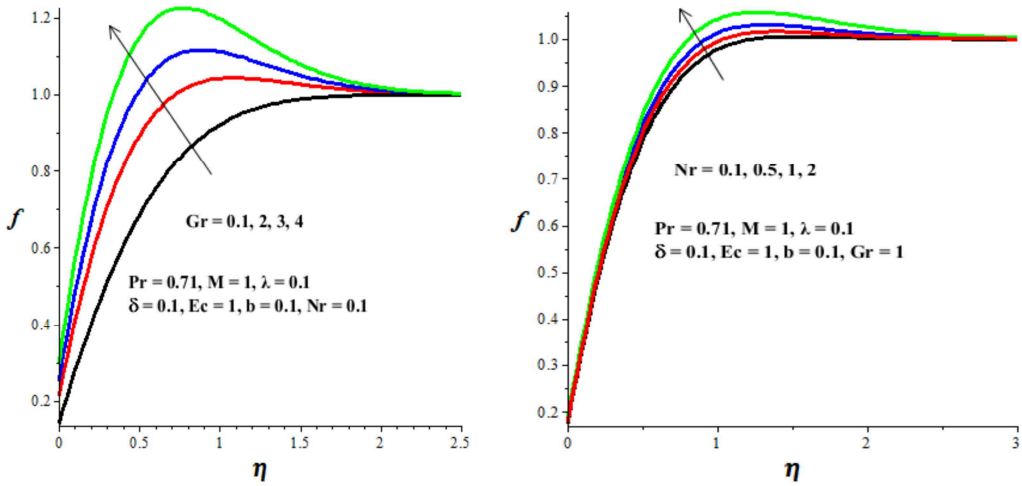
Velocity Profiles

Figures 2-10 depict the effects of various thermophysical parameters on the longitudinal velocity profiles and the momentum boundary layer thickness. Generally, the fluid velocity is zero at the permeable stationary plate surface and increases to the prescribed free stream value satisfying the far field boundary condition. In figures 2-6, a decrease in the momentum boundary layer thickness accompanies an increase in the magnetic field intensity parameter (M), suction parameter (b>0), Grashof number (Gr), radiation absorption parameter (Nr) and Eckert number (Ec) with all profiles tending asymptotically to the free stream value away from the plate. Consequently, the fluid

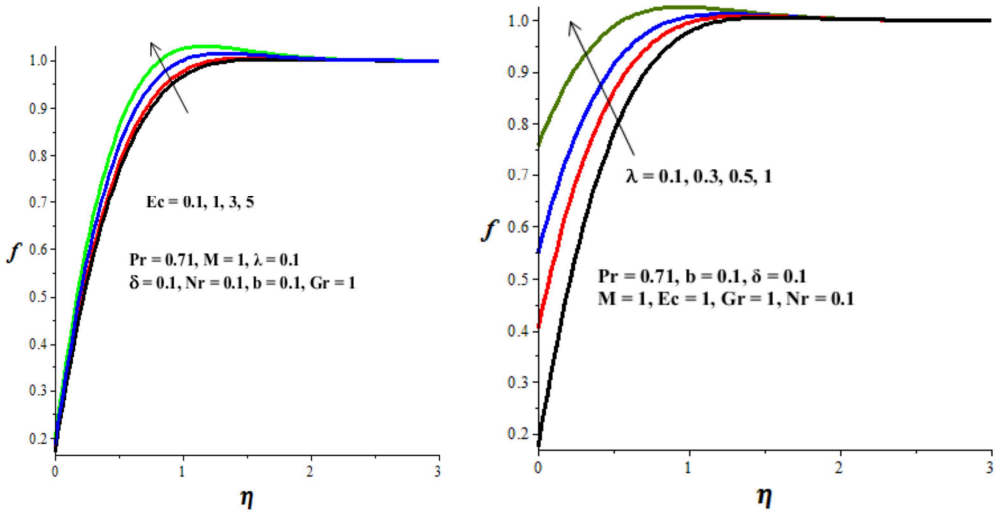
motion in the boundary layer region adjacent to the plate surface increases. This implies that the electrically conducting fluid receives a push from the electromagnetic Lorentz force towards the permeable plate surface. This is the reason why the magnetic field has the potential to move forward an electrically conducting fluid in the microscale system. Similarly, it is noteworthy that fluid suction, radiation absorption and buoyancy force due to temperature difference also pushes the fluid towards the plate surface in the same manner. Figure 7 shows the effect of velocity slip on the plate surface. It is noted that an increase in slip parameter λ corresponds to a rise in the fluid velocity adjacent to the surface. In figures 8-10, we observed that the momentum boundary layer thickness increases with an increase in fluid injection (b<0), temperature jump parameter (δ) and the Prandtl number (Pr). This may be attributed to the combined effects of additional heated fluid entering into the flow regime through injection and a decrease in the fluid thermal diffusivity.



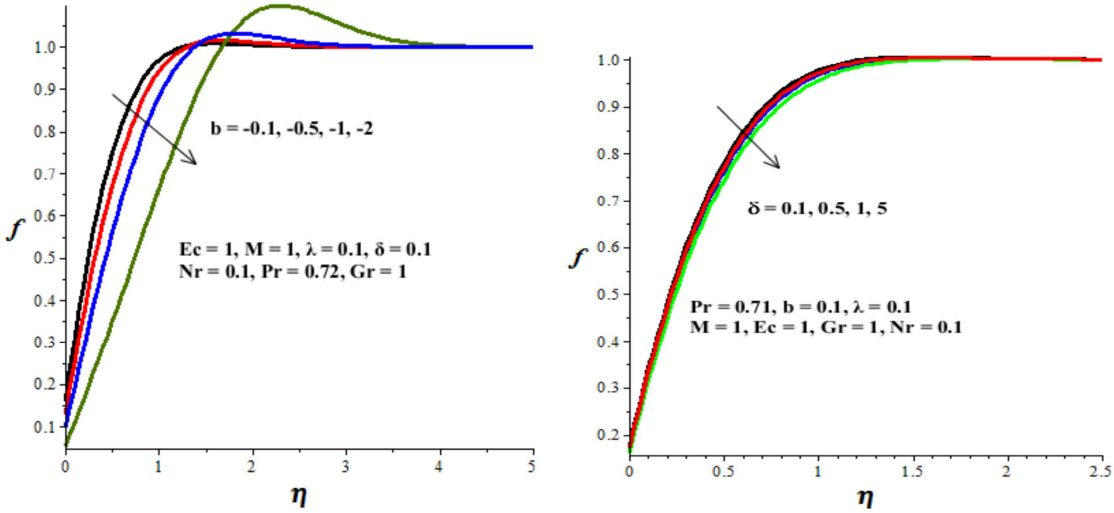
Figs.2-3: Velocity profile with increasing M and b>0.



Figs.4-5: Velocity profile with increasing Gr and Nr.



Figs.6-7: Velocity profile with increasing Ec and λ.



Figs.8-9: Velocity profile with increasing injection b<0 and δ.

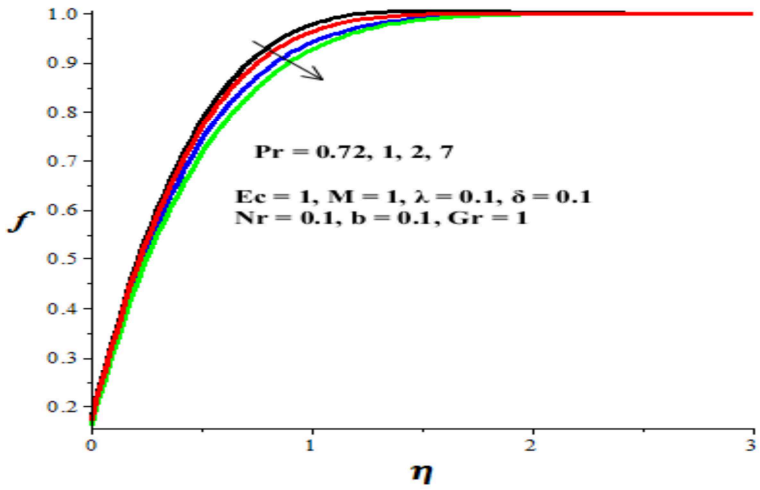
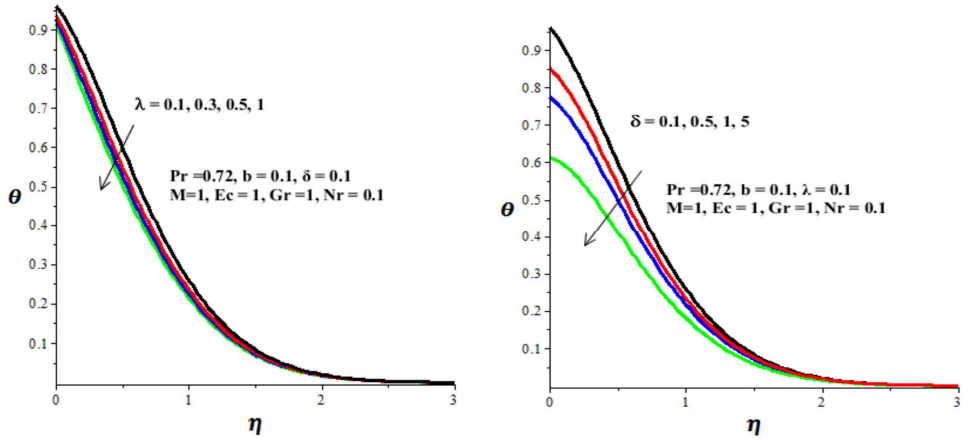


Fig. 10: Velocity profile with increasing Pr.

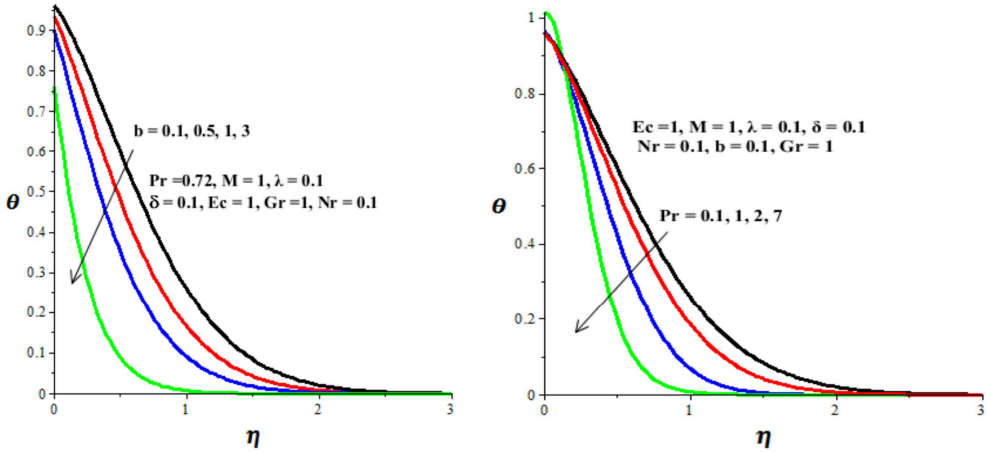
Temperature Profiles

Figures 11-19 illustrate the effects of parameters variations on temperature distribution.The fluid temperature is highest at the plate surface and decreases exponentially to the free steam zero value satisfying the prescribed far field condition. We observed that the thermal boundary layer

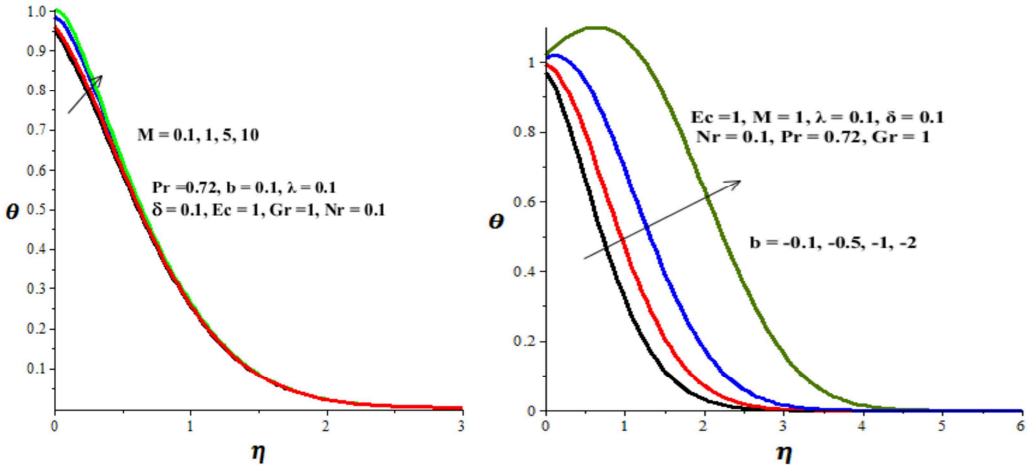
thickness decreases with an increase in velocity slip parameter (λ), temperature jump parameter (δ), fluid suction ($b > 0$) and Prandtl number (Pr) as shown in figures 11-14, consequently, the plate surface temperature also decreases. It is important to note that increase in δ correspond to a convective cooling of the plate surface. Figure 15 depicts a rise in the fluid temperature and thermal boundary layer thickness as the magnetic field intensity parameter increases. The presence of Joule heating (or Lorentz heating due to magnetic field) serves as an additional heat source to the flow system leading to an elevation in the fluid temperature. Similar trend of a rise in the fluid temperature and thermal boundary layer thickness is observed in figures 16-19 with an increase in fluid injection parameter ($b < 0$), Grashof number (Gr), radiation absorption parameter (Nr) and Eckert number (Ec). This increase in fluid temperature can be attributed to the absorption of heat by the fluid from the plate surface leading to surface cooling and the viscous dissipation effect that contribute additional heat source to the flow.



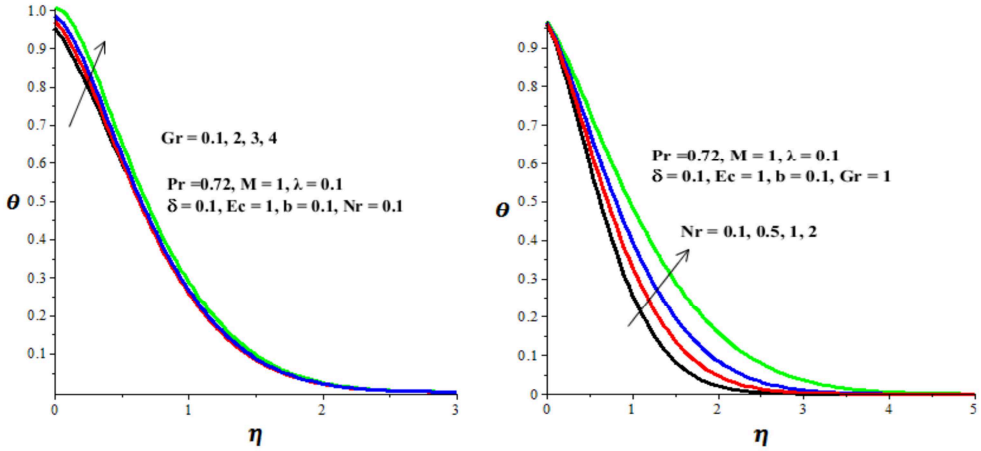
Figs.11-12: Temperature profiles with increasing λ and δ.



Figs. 13-14: Temperature profiles with increasing suction ($b > 0$) and Pr.



Figs.15-16: Temperature profiles with increasing *M* and b<0.



Figs. 17-18: Temperature profiles with increasing Gr and Nr.

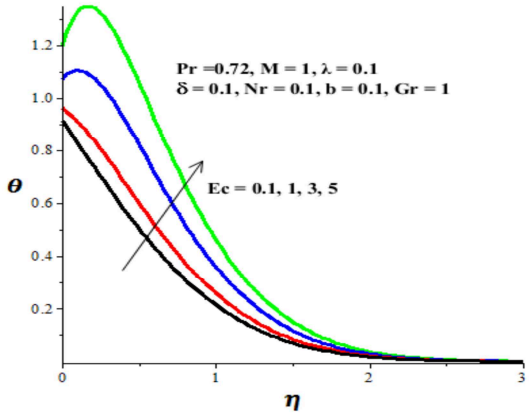
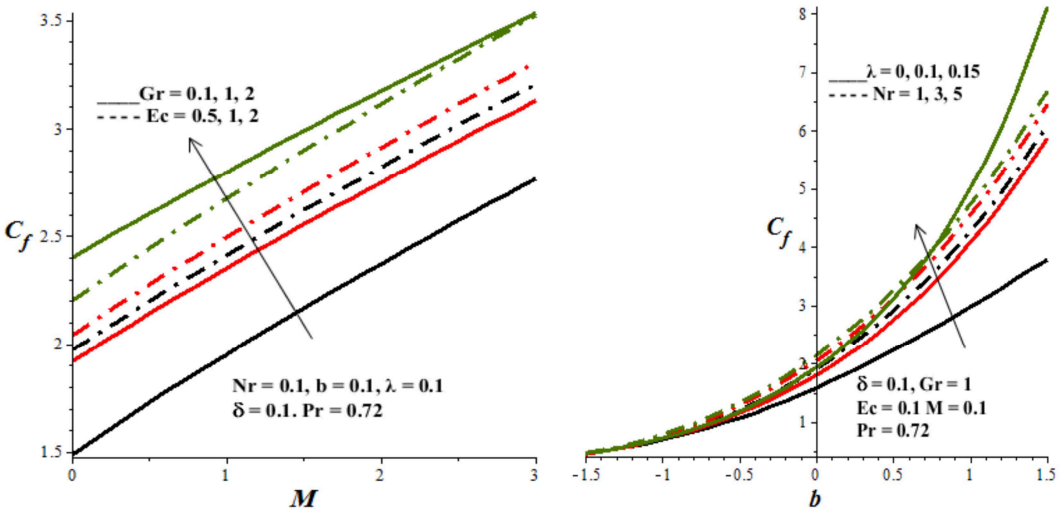


Fig.19: Temperature profiles with increasing *Ec*.

Skin Friction and Nusselt Number

Figures 20-25 give the distribution of the skin friction coefficient and Nusselt number at the plate surface for various thermophysical parameter values. One can note from figure 20 that the skin friction coefficient increases with an increase in magnetic field intensity (*M*), Grashof number (*Gr*) and Eckert number (*Ec*). This may be attributed to a rise in the velocity gradient at the plate surface due to momentum gain produced by Lorentz force, thermal buoyancy and viscous dissipation in boundary layer. Figures 21-22 show that the skin friction coefficient increases with an increase in fluid suction, velocity slip and thermal radiation absorption but decreases with an increase in fluid

injection, temperature jump and Prandtl number. This increase or decrease in the skin friction coefficients can be attributed to a decrease or increase in the velocity gradient at the plate surface as these parameters increase. Moreover, it is noted that, in the slip flow regime, shear stress adjacent to the surface can be manipulated through suction/injection parameter. Figures 23-25 exhibit the effects of thermophysical parameters variation on the plate surface heat transfer rate. An increase in the magnetic field intensity (*M*), Grashof number (*Gr*) and Eckert number (*Ec*) causes a decrease in the surface heat transfer rate as shown in figure 23. This is expected, since a rise in the fluid temperature due to *M*, *Gr* and *Ec* increase causes a decrease in the temperature gradient at the plate surface, consequently, the Nusselt number decreases. Figure 24 revealed that an increase in mass suction tend to increase surface heat transfer rate whereas injection acts in the opposite way. Moreover, the Nusselt number reduces with an increase in both slip coefficient and temperature jump parameter due to surface cooling. It is interesting to note that the hydrodynamic slip and temperature jump boundary conditions have capability of decreasing the heat transfer rate along stationary permeable surface. Figure 25 shows a rise in the surface heat transfer rate as the thermal radiation absorption parameter (*Nr*) and Prandtl number (*Pr*) increase. As expected, increase in Nr represents a rise in the radiative heat transfer which contributes to the total heat transfer rate at the plate surface. However, a decrease in the fluid temperature due to *Pr* causes an increase in the temperature gradient at the plate surface, consequently, the Nusselt number increases.



Figs.20-21: Skin friction with increasing *Ec*, *Gr*, *M*, Nr, b and *λ*.

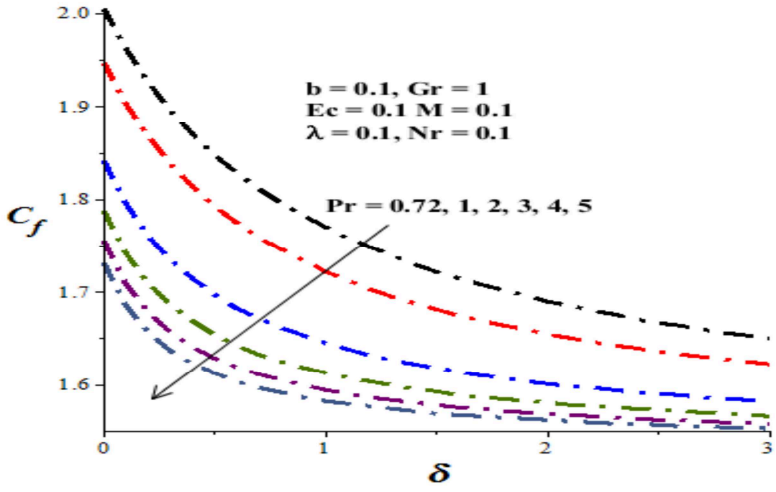
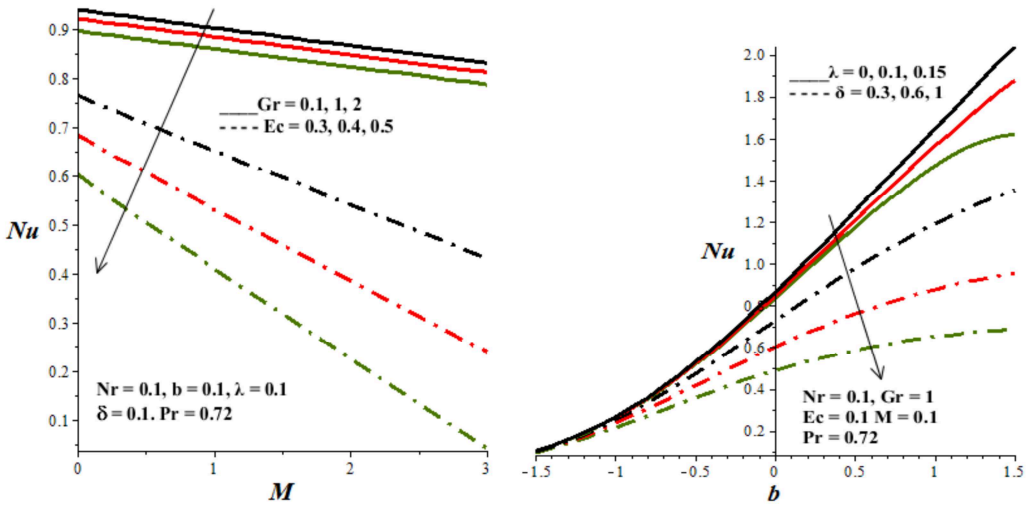


Fig.22: Skin friction with increasing *Pr* and *δ*.



Figs.23-24: Nusselt number with increasing *Gr*, *Ec*, *M*, λ, δ and *b*.

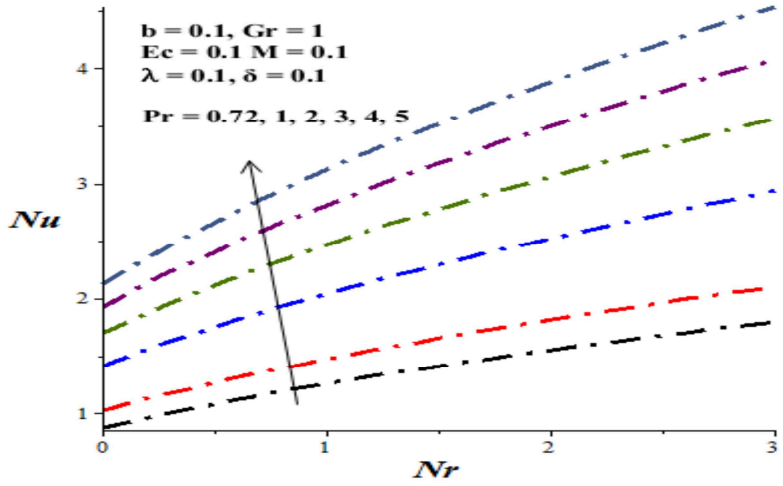
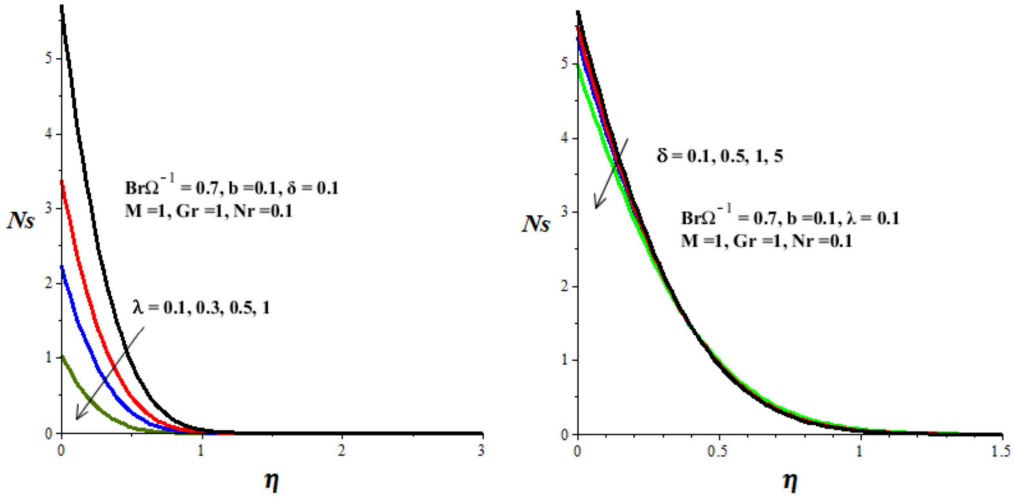


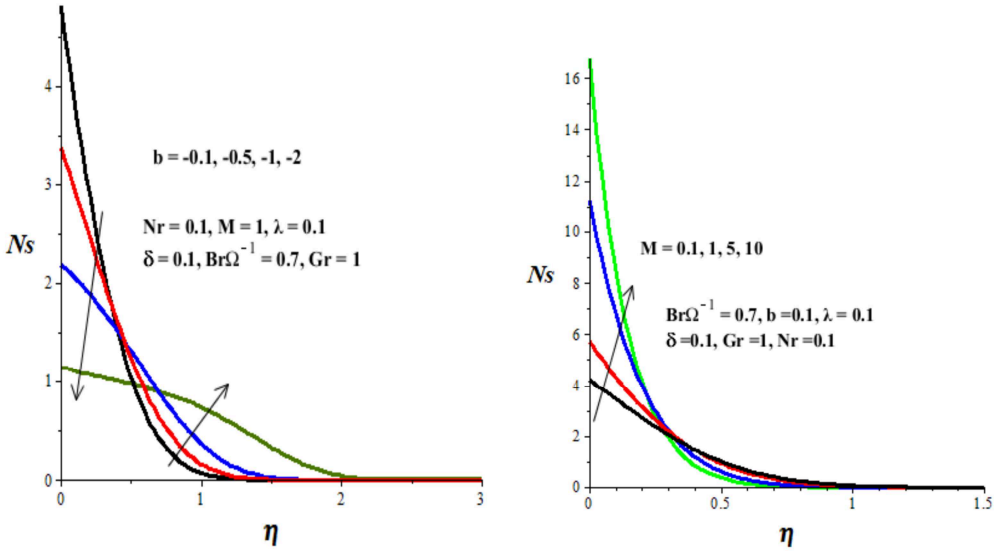
Fig. 25: Nusselt number with increasing *Nr* and *Pr*.

Entropy Generation Rate

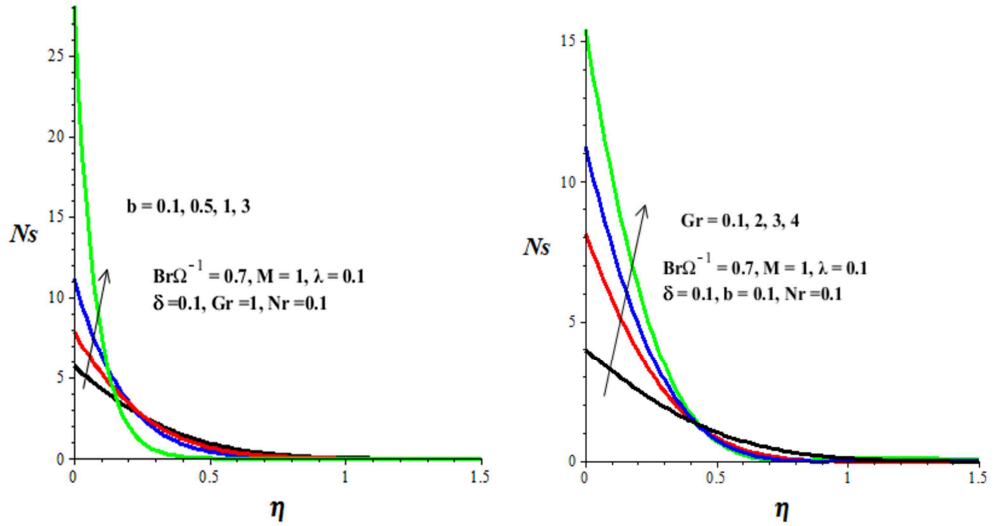
Figures 26-33 display the entropy generation rate for various parametric values. Generally, the entropy production attained its highest value at the permeable plate surface and gradually decreases to zero value at free stream far away from the plate surface. Interestingly, an increase in the slip coefficient, temperature jump parameter and fluid injection decreases the entropy production at the plate surface and within the boundary layer as shown in figures 16-28. Moreover, the slip coefficient, temperature jump parameter and fluid injection have decreasing effects on both fluid friction and heat transfer irreversibilities. The effect of the magnetic field parameter *M* on the entropy generation rate is shown in figure 29. It is indicated that an increase in the *M* tends to increase the entropy production at the plate surface and within boundary layer region. This can be attributed to the fact that the magnetic field parameter has an increasing effect on the fluid friction and magnetic irreversibilities. Similar trend is observed in figures 29-33. As the values of fluid suction parameter ($b > 0$), Grashof number (*Gr*), radiation absorption parameter (*Nr*) and dimensionless group parameter ($Br\Omega^{-1}$) increase, the entropy production at the plate surface and within the boundary layer increases. It is important to note that Grashof number (*Gr*), suction ($b > 0$) and dimensionless group parameter $Br\Omega^{-1}$ have increasing effects on fluid friction and magnetic irreversibilities while the radiation absorption (*Nr*) has increasing effect on the heat transfer irreversibility.



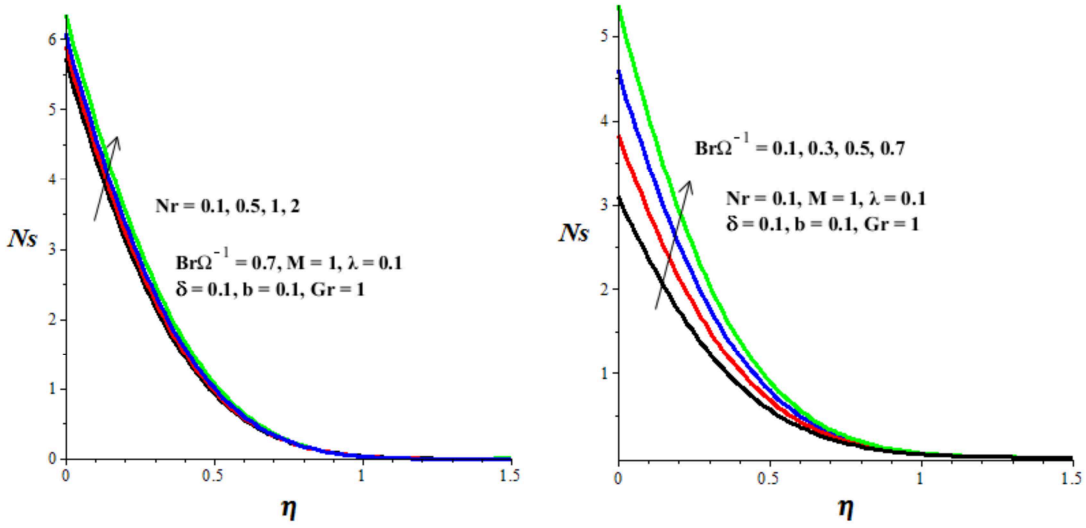
Figs.26-27: Entropy generation rate with increasing λ and δ.



Figs.28-29: Entropy generation rate with increasing injection (b<0) and M.



Figs.30-31: Entropy generation rate with increasing suction (b>0) and Gr.



Figs.32-33: Entropy generation rate with increasing *Nr* and $Br\Omega^{1}$.

Bejan Number

Figures 34-41 illustrate the effects of parameter variation on Bejan (*Be*) number. Generally, Bejan number ranges from 0 to 1. It is interesting to note that the irreversibility is solely due to thermal radiation absorption and heat transfer at the free stream with Bejan number approaches 1 for all parameter values, while at the permeable plate surface, the Bejan number is much less than 1 and in some cases approaches zero. This implies that the irreversibilities due to the combined effects of fluid friction and magnetic field increase their dominant at the plate surface. Moreover, as the value of slip coefficient increases (λ), the dominant effects of fluid friction and magnetic field irreversibilities at the plate surface decrease and the value of Bejan number increases above zero (see figure 34). The irreversibility due to thermal radiation absorption and heat transfer dominates when $Be > 0.5$. Similar trend is observed in figure 35 with increasing Bejan number ($Be > 0$) at the plate surface as suction parameter increases. Figure 36-39 show the combined effects of dimensionless group parameter ($Br\Omega^{1}$), temperature jump parameter (δ), radiation absorption parameter (*Nr*) and fluid injection parameter ($b < 0$) on the Bejan number at the plate surface and within the boundary layer region. It is observed that as these parameters increase, the Bejan number at the plate surface tends to zero, consequently, the entropy generation due to the combined effects of fluid friction and magnetic field are dominant. It can also be observed from figures 40-41 that the Bejan number decreases to zero at the plate surface with increasing magnetic field intensity (*M*) and thermal buoyancy (*Gr*), consequently, fluid friction and magnetic field irreversibilities dominate. Finally, it is noteworthy that the plate surface acts as a strong source of irreversibility. The entropy generation within the boundary layer region can be attributed to the combined action of thermal radiation, heat transfer, fluid friction and magnetic field irreversibilities.

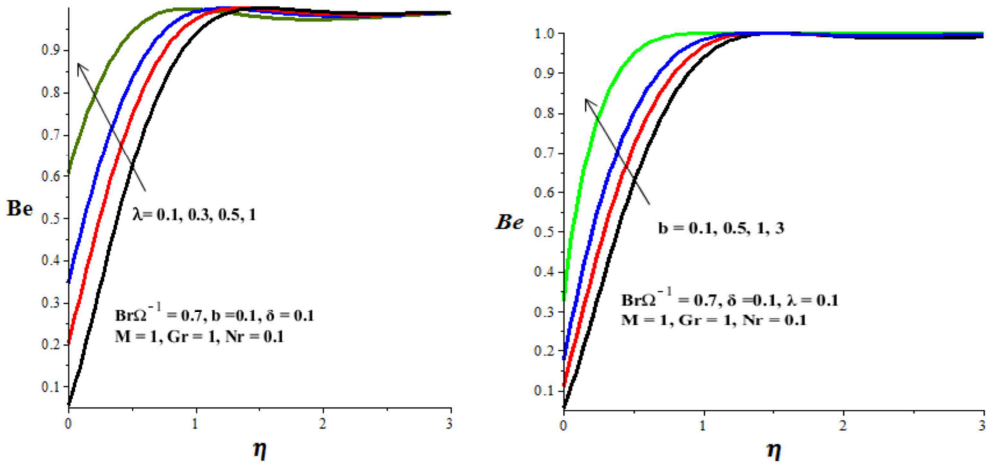
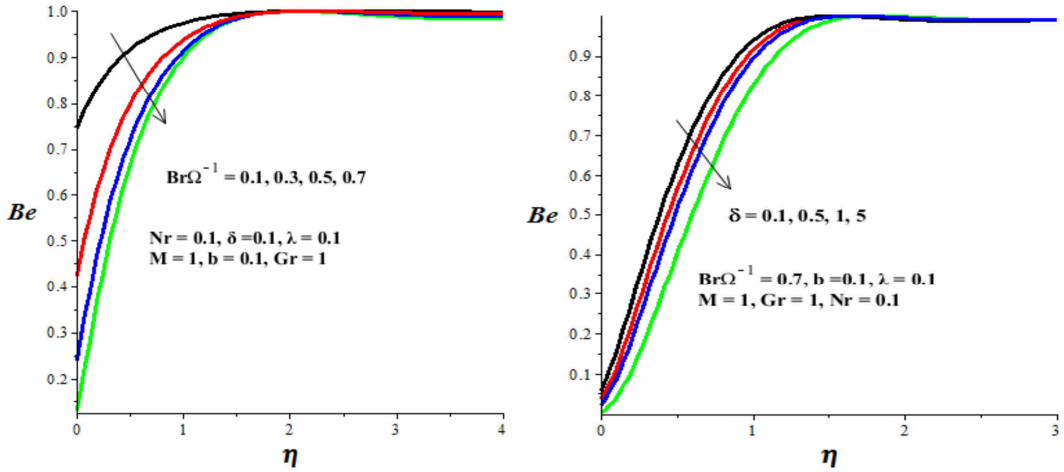
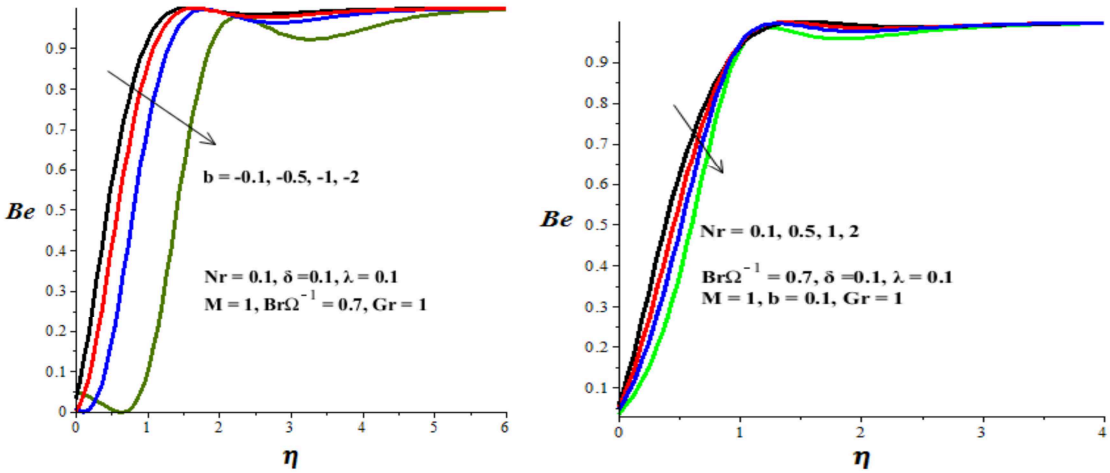


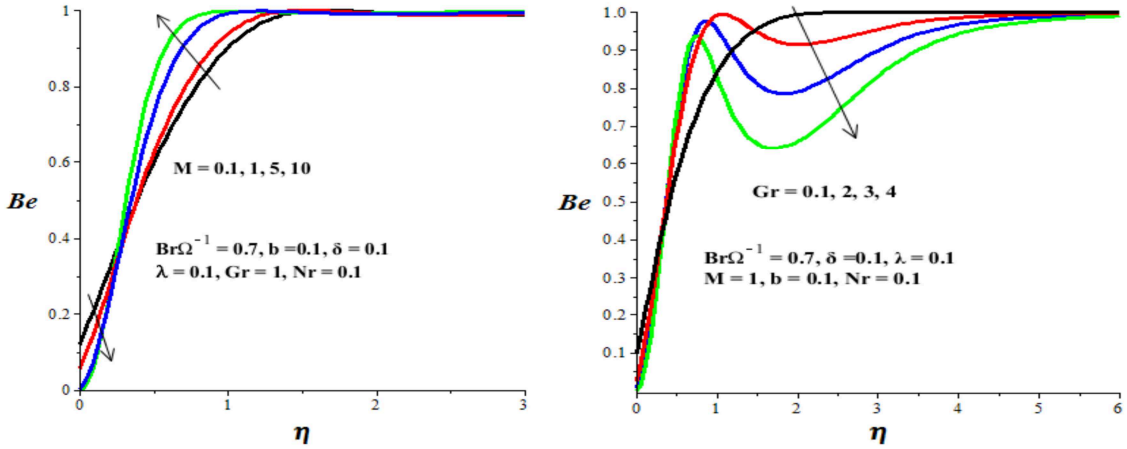
Fig. 34-35: Bejan number with increasing λ and $b>0$.



Figs. 36-37: Bejan number with increasing $Br\Omega^{-1}$ and δ.



Figs. 38-39: Bejan number with increasing Nr and $b < 0$.



Figs.40-41: Bejan number with increasing M and Gr.

Conclusions

The entropy generation rate in an unsteady mixed convection flow of an electrically conducting and thermally radiating fluid past a permeable vertical surface subjected to a combined action of a transverse magnetic field, Joule heating, viscous dissipation, buoyancy force, velocity slip and temperature jump is analysed. The prescribed free stream velocity outside the boundary layer is also affected by magnetic field; consequently, the Lorenz force can push the fluid forward to accelerate the fluid motion. Using similarity variable, the model partial differential equations are transformed to a set of nonlinear coupled ordinary differential equations and solved numerically using shooting technique coupled with Runge-Kutta Fehlberg integration technique. Graphical results are presented for the fluid velocity and temperature profiles, local skin friction coefficient and local Nusselt number, entropy generation rate and Bejan number. The main findings can be summarized as follows:

- The momentum boundary layer thickness increases with an increase in Pr, δ and $b < 0$ but decreases with an increase in M, Gr, Nr, Ec, λ and $b>0$.
- The thermal boundary layer thickness increases with an increase in M, Gr, Nr, Ec and b<0 but decreases with an increase in λ, δ, Pr and $b>0$.
- The local skin friction coefficient increases with an increases in M, Gr, Nr, Ec, λ and $b > 0$, but decreases with an increase in Pr, δ and $b < 0$.
- The local Nusselt number increases with an increases in Pr, Nr and $b > 0$, but decreases with an increase in M, Gr, δ, Ec, λ and $b<0$.
- The entropy production at the plate surface increases with an increase in M, Gr, Nr, $Br\Omega^{-1}$ and $b > 0$ but decreases with an increase in δ, λ and $b < 0$.
- Heat transfer irreversibility solely dominate the free stream with Bejan number of 1 while at the plate surface the irreversibilities due to both fluid friction and magnetic field dominates with Bejan number approaching zero as $b < 0$, M, δ, Gr, Nr, $Br\Omega^{-1}$ increasing and λ, $b > 0$ decreasing.

Finally, it is evident that the entropy generation rate in unsteady hydromagnetic mixed convective flow over a permeable slippery surface with thermal radiation can be sufficiently reduced using appropriate combination of thermophysical parameter values for efficient operation. Moreover, the above results can be applied to improve the design of a variety of flow and thermal systems including micro scale systems such as micromixing technologies. It is hoped that the present work will serve as a stimulus for experimental work which appears to be lacking at present.

References

[1] A. Nisar, N. Afzulpurkar, B. Mahaisavariya, A. Tuantranont, MEMS-based micropumps in drug delivery and biomedical applications. Sens. Actuators B Chem. 130 (2008) 917–942.

[2] L. Capretto, W. Cheng, M. Hill, X. Zhang, Micromixing within microfluidic devices. Top. Curr. Chem., 304 (2011) 27–68.

[3] C. Kleinstreuer, J. Li, J. Koo, Microfluidics of nano-drug delivery. Int. J. Heat Mass Trans., 51 (2008) 5590–5597.

[4] D. C. Tretheway, C. D. Meinhart, A generating mechanism for apparent fluid slip in hydrophobic microchannels. Phys. Fluids, 16 (2004) 1509–1515.

[5] E. M. Sparrow, E. R. Eckert, W. J. Minkowycz, Transpiration cooling in a magnetohydrodynamic stagnation-point flow. Appl Sci Res A 11 (1962) 125–147.

[6] S. Rosseland, Theoretical astrophysics. Oxford University, New York, NY, USA, 1936.

[7] O. D. Makinde, A. Ogulu, The effect of thermal radiation on the heat and mass transfer flow of a variable viscosity fluid past a vertical porous plate permeated by a transverse magnetic field. Chemical Engineering Communications,195 (12) (2008) 1575 -1584.

[8] O. D. Makinde, Free-convection flow with thermal radiation and mass transfer past a moving vertical porous plate. International Communications in Heat and Mass transfer, 32 (2005) 1411-1419.

[9] K. R. Cramer, S. I. Pai, Magnetofluid dynamics for engineers and applied physicists. McGraw–Hill, New York, 1973.

[10] O. D. Makinde, O. O. Onyejekwe, A numerical study of MHD generalized Couette flow and heat transfer with variable viscosity and electrical conductivity. Journal of Magnetism and Magnetic Materials, 323 (2011) 2757–2763.

[11] O. D. Makinde, T. Chinyoka, Numerical investigation of buoyancy effects on hydromagnetic unsteady flow through a porous channel with suction/injection. Journal of Mechanical Science and Technology, 27 (5) (2013) 1557-1568.

[12] O. D. Makinde, W. A. Khan, J. R. Culham, MHD variable viscosity reacting flow over a convectively heated plate in a porous medium with thermophoresis and radiative heat transfer. International Journal of Heat and Mass Transfer, 93 (2016) 595–604.

[13] S. Mukhopadhyay, Slip effects on MHD boundary layer flow over an exponentially stretching sheet with suction/blowing and thermal radiation. Ain Shams Eng. J., 4(3) (2013) 485-491.

[14] P. R. Sharma, G. Singh, Effects of variable thermal conductivity, viscous dissipation on Steady MHD natural convection flow of low Prandtl fluid on an inclined porous plate with Ohmic heating. Meccanica, 45 (2010) 237- 247.

[15] Y. J. Kim, Unsteady MHD convective heat transfer past a semi-infinite vertical porous moving plate with variable suction. International Journal of Engineering Science, 38 (2000) 833-845.

[16] K. Bhattacharyya, G. C. Layek, Chemically reactive solute distribution in MHD boundary layer flow over a permeable stretching sheet with suction or blowing. Chem. Eng. Commun., 197 (2010) 1527-1540.

[17] L. Zheng, J. Niu, X. Zhang, Y. Gao, MHD flow and heat transfer over a porous shrinking surface with velocity slip and temperature jump. Math. Comp. Model., 56 (2012), 133-144.

[18] N. Kishan, S. Jagadha, Influence of thermophoresis on heat and mass transfer under non-Darcy MHD mixed convection along a vertical flat plate embedded in a porous medium in the presence of radiation. Thermophys. Aeromech. 23(1) (2016) 97-108.

[19] D. Hunegnaw, N. Kishan, Scaling group analysis on MHD effects on heat transfer near a stagnation point on a linearly stretching sheet with variable viscosity and thermal conductivity, viscous dissipation and heat source/sink. Theoretical and Applied Mechanics, 42(2) (2015) 111–133.

[20] D. Hunegnaw, N. Kishan, Unsteady MHD flow of heat and mass transfer of nanofluids over stretching sheet with a non-uniform heat/source/sink considering viscous dissipation and chemical reaction. International Journal of Engineering Research in Afrika, 14 (2015) 1-12.

[21] P. Kavitha, N. Kishan, MHD flow of a non-Newtonian power-law fluid over a stretching sheet with thermal radiation, viscous dissipation and slip boundary conditions. Acta Technica, 59(4) (2014) 355–376.
[22] E. H. Lieb, J. Yngvason, The physics and mathematics of the second law of thermodynamics. Physics Reports, 310 (1999) 1–96.
[23] A. Bejan, A., A study of entropy generation in fundamental convective heat transfer. J. Heat Transfer, 101 (1979) 718-725.
[24] A. Bejan, A., Tsatsaronis, G., Moran, M., Thermal design and optimization, Wiley, New York, USA, 1996.
[25] O. D. Makinde, Entropy analysis for MHD boundary layer flow and heat transfer over a flat plate with a convective surface boundary condition. Int. J. Exergy, 10 (2) (2012) 142-154.
[26] S. Das, S. Chakraborty, R. N. Jana, O. D. Makinde, Entropy analysis of unsteady magneto-nanofluid flow past accelerating stretching sheet with convective boundary condition. Applied Mathematics and Mechanics, 36 (12) (2015) 1593-1610.
[27] G. Ibáñez, S. Cuevas, Entropy generation minimization of a MHD flow in a microchannel. Energy, 35 (2010) 4149–4155.
[28] L. C. Woods, Thermodynamics of fluid systems. Oxford University Press, Oxford, UK, 1975.
[29] T. Chinyoka, O. D. Makinde, Analysis of entropy generation rate in an unsteady porous channel flow with Navier slip and convective cooling. Entropy, 15 (2013) 2081-2099.
[30] S. Mahmud, R. A. Fraser, Flow, thermal and entropy generation characteristic inside a porous channel with viscous dissipation. Int. J. Therm. Sci. 44 (2005), 21-32.
[31] O. D. Makinde, O. A. Beg, On inherent irreversibility in a reactive hydromagnetic channel flow. Journal of Thermal Science 19 (1) (2010), 72-79, 2010.
[32] O. D. Makinde, Entropy analysis for MHD boundary layer flow and heat transfer over a flat plate with a convective surface boundary condition. International Journal of Exergy, 10 (2) (2012) 142-154.
[33] M. H. Yazdi, S. Abdullah, I. Hashim, K. Sopian, Reducing entropy generation in MHD fluid flow over open parallel microchannels embedded in a micropatterned permeable surface. Entropy, 15(2013) 4822-4843.
[34] T.Y. Na, Computational methods in engineering boundary value problem. Academic Press, 1979.